Available online at www.sciencedirect.com
ScienceDirect
Journal of Photochemistry and Photobiology A: Chemistry 197 (2008) 426–433
Journal of Photochemistry and Photobiology A:Chemistry
www.elsevier.com/locate/jphotochem

Sul-containing fluorinated polyimides for optical waveguide device

Wei Jiang [a], Dong Wang [a], Shaowei Guan [a], Hong Gao [a], Yili Zhao [a], Zhenhua Jiang [a,*], Weinan Gao [b], Dan Zhang [b], Daming Zhang [b]

[a] *Alan G. MacDiarmid Institute of Jilin University, Changchun 130023, PR China*
[b] *State Key Laboratory on Integrated Optoelectronics, Jilin University Region, Changchun 130023, PR China*

Received 9 December 2007; received in revised form 16 January 2008; accepted 7 February 2008
Available online 14 February 2008

Abstract

Novel sul-containing fluorinated polyimides have been synthesized by the reaction of 2,2′-bis-(trifluoromethyl)-4,4′-diaminodiphenyl sulfide (TFDAS) with 1,4-bis-(3,4-dicarboxyphenoxy)benzene dianhydride (HQDPA), 2,2′-bis-(3,4-dicarboxyphenyl)hexafluoropropane dianhydride (6FDA), 4,4′-oxydiphthalicanhydride (ODPA) or 3,4,3′,4′-biphenyl-tetracarboxylic acid dianhydride (*s*-BPDA). The fluorinated polyimides, prepared by a one-step polycondensation procedure, have good solubility in many solvents, such as *N*-methyl-2-pyrrolidinone (NMP), dimethylacetamide (DMAc), dimethyl sulfoxide (DMSO), cyclohexanone, tetrahydrofuran (THF) and *m*-cresol. The molecular weights (M_n's) and polydispersities (M_n/M_w's) of polyimides were in the range of 1.24×10^5 to 3.21×10^5 and 1.59–2.20, respectively. The polymers exhibit excellent thermal stabilities, with glass-transition temperatures (T_g) at 221–275 °C and the 5% weight-loss temperature are above 531 °C. After crosslinking, these polymers show higher thermal stability. The films of polymers have high optical transparency. The novel sul-containing fluorinated polyimides also have low absorption at both 1310 and 1550 nm wavelength windows. Rib-type optical waveguide device was fabricated using the fluorinated polyimides and the near-field mode pattern of the waveguide was demonstrated.

Keywords: Optical waveguide; Fluorinated polyimide; Sulfur

1. Introduction

Polymer optical waveguides have attracted considerable attention for their possible application as optical components in optical interconnects and optical communication systems because of their potential ease of manufacture at low temperature, and the low cost of processing [1].

The key issues on the polymer waveguide materials include four aspects: (1) low propagation losses at the optical communication wavelengths, (2) high thermal stability to provide compatibility with high-performance electronic device fabrication, (3) controllability of refractive index for the easy control of the waveguide dimension to match the mode size with fibers, and (4) good adhesion to the silicon substrate [2–5]. However, hydrocarbon polymers have a high optical loss in the infrared communication region due to carbon–hydrogen (C–H) bond vibrational absorption. By modifying a molecule via the substitution of fluorine or deuterium for hydrogen in the C–H greatly reduces optical loss. Many organic polymers such as deuterated or fluorinated poly(methyl methacrylate) (PMMA) [6,7], polystyrene (PS) [8,9], and poly(carbonate) (PC) [10,11] are used as materials for a variety of optical components. However, these polymers do not have sufficient thermal stability at high temperature, for the fabrication temperature of the optical devices is 260 °C, and the short time temperature is up to 400 °C. Fluorinated polyimides are more accessible than these polymers because of their molecular structure. In addition, they have good thermooxidative stability, outstanding mechanical properties, fire resistance and so on [12–15]. However, polyimides due to their stiff backbone need improvements to lower the birefringence.

Moreover, sul-containing aromatic polymers such as polysulfide and polysulfone are key polymers for optical materials because of their high atomic refraction of the sulfur atom [16–18]. Further sul-containing aromatic polymers have great thermal stability for the existence of 3d orbit sulfur atom.

* Corresponding author. Tel.: +86 431 85168886; fax: +86 431 85168886.
E-mail addresses: jiangwei@email.jlu.edu.cn (W. Jiang), jiangzhenhua@jlu.edu.cn (Z. Jiang).

1010-6030/$ – see front matter © 2008 Elsevier B.V. All rights reserved.
doi:10.1016/j.jphotochem.2008.02.005

In this study, we introduced the sulfur atom to the famous fluorinated polyimide monomer 2,2′-bis-(trifluoromethyl)-4,4′-diaminobiphenyl (TFDB) [19,20], and hope the new material can keep the advantage of the famous polyimide. The sulfide groups in polymers were introduced to improve adhesion to the Si substrates [5]. Furthermore, sulfur atom can act as a potential crosslinking group while fabricating optical waveguide devices. It can be heated or irradiated to crosslink to satisfy the need of the interbedded technology of the devices [21–24]. After crosslinking, these polymers show higher thermal stability. The sulfide crosslinking will not introduce C–H bond compared to the other common crosslinking groups [5,25], thus it can decrease the C–H bond vibrational absorption and lower optical loss will be expected. The novel polyimides were charactered in detail for properties and also applied to fabricate optical waveguide devices. The optical properties of the device are also demonstrated.

2. Experimental

2.1. Materials

1,4-Bis-(3,4-dicarboxyphenoxy)benzene dianhydride (HQDPA) was purchased from Changchun Institute of Applied Chemistry, Chinese Academy of Science and recrystallized from acetic anhydride before used. 4,4′-(Hexafluoroisopyrilidene)diphthalic anhydride (6FDA) was purchased from Aldrich Chemical Co. and baked at 160 °C in vacuo overnight before use. 4,4′-Oxydiphthalicanhydride (ODPA) and 3,4,3′,4′-biphenyl-tetracarboxylic acid dianhydride (*s*-BPDA) were purchased from Aldrich Chemical Co. and recrystallized from acetic anhydride before use. *N*,*N*-Dimethylacetamide (DMAc) was purified by distillation under reduced pressure over calcium hydride and stored over molecular sieves. Other chemicals were used as received.

2.2. Measurements

The differential scanning calorimetry (DSC) was performed on a Mettler Toledo DSC821e at a rate of 20 °C/min under a nitrogen atmosphere. The thermogravimetric analysis (TGA) was performed using a PerkinElmer TGA-7 thermal analyzer system at the heating rate of 10 °C/min under nitrogen. The FTIR spectra (KBr or film) were measured using a Nicolet Impact 410 Fourier transform infrared spectrometer. Gel permeation chromatograms (GPC) were obtained by a Waters 410 instrument with tetrahydrofuran (THF) as the eluent and polystyrene as the standard. The ^{1}H NMR (500 MHz) spectra were recorded using a Bruker 510 NMR spectrometer with tetramethylsilane as the reference. The birefringence of the polymer films, at the 650 nm wavelength, were determined from coupling angles of TE (transverse electric) or TM (transverse magnetic) optical guided modes with a gadolinium gallium garnet (GGG) prism. The UV–vis absorption spectra were recorded on a UV2501-PC spectrophotometer. The SEM measurement was performed on a SHIMADZU SSX-550 microscope. Near-infrared spectra (near-IR) were performed on a Varian Kera 500 spectrometer. Refractive indices of polymer films were measured by M-2000UI spectroscopic ellipsometer (J.A. Woollam, Lincoln, USA). The atomic force microscopy (AFM) observations of the surface were carried out with the commercial instrument (Digital Instrument, Nanoscope IIIa, Multimode). All the tapping mode images were taken at room temperature in air with the microfabricated rectangle crystal silicon cantilevers (Nanosensor). The topography images were obtained at a resonance frequency of approximately 365 kHz for the probe oscillation.

2.3. Synthesis of monomer

The monomer, TFDAS was synthesized several years ago [26]. In this paper, we used a different method to obtain the final monomer, and the procedure is described in Scheme 1.

A mixture of 2-chloro-5-nitrobenzotrifluoride (11.75 g, 50 mmol), sodium sulfide 9-hydrate (6 g, 25 mmol) and 50 mL DMAc was placed in a 100-mL, three-necked, round-bottom flask equipped with a mechanical stirrer, a reflux condenser, and a nitrogen purge. The mixture was refluxed with stirring for 8–12 h and then cooled to room temperature. The mixture was poured into an ethanol/water (1:5, v/v) mixture to give a yellow solid material, which was collected and washed with cold ethanol and water then dried at 100 °C in vacuo.

m.p.: 136 °C. FTIR (KBr): 1533, 1350, 1303, 1128, 1030, 740 cm^{-1}. ^{1}H NMR (500 MHz, $CDCl_3$, δ, ppm): 8.66 (s, 2H), 8.32 (d, J = 8.5 Hz, 2H), 7.42 (d, J = 9.0 Hz, 2H).

A slurry of 2,2′-bis-(trifluoromethyl)-4,4′-dinitrodiphenyl sulfide (31.724 g, 77 mmol), stannous chloride ($SnCl_2$) (59.75 g, 315 mmol) and 280 mL of anhydrous EtOH was stirred while 208 mL of concentrated HCl was added slowly. After addition of HCl was over, the mixture was refluxed for 8 h. Excess EtOH was evaporated and the remaining solution was poured into 280 mL ice–water mixture. The solution was basified with 10% NaOH solution and the pale yellow precipitate was filtered off, washed repeatedly with hot water and dried in vacuo. The sample was recrystallized from aqueous alcohol.

m.p.: 74 °C. FTIR (KBr): 3500, 3544, 3361, 3224, 1347, 1029 cm^{-1}. ^{1}H NMR (500 MHz, DMSO, δ, ppm): 6.96 (s, 2H), 6.91 (d, J = 8.5 Hz, 2H), 6.71 (d, J = 8.5 Hz, 2H), 5.76 (s, 4H).

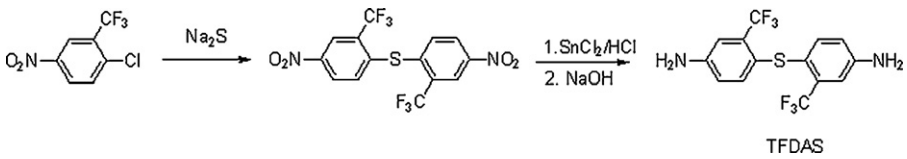

Scheme 1. Synthesis of 2,2′-bis-(trifluoromethyl)-4,4′-diaminodiphenyl sulfide.

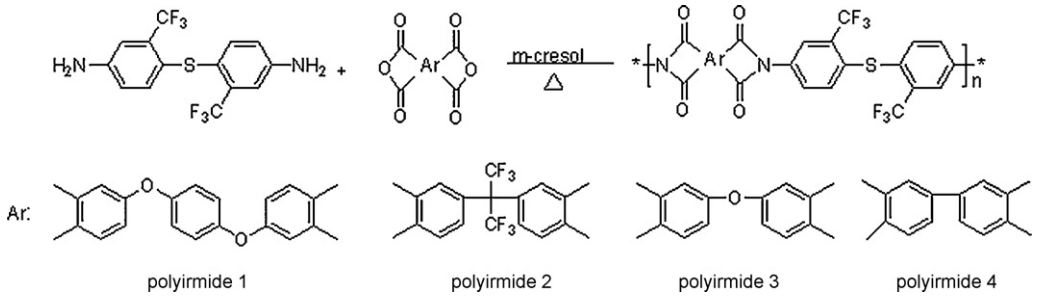

Scheme 2. Synthesis of sul-containing fluorinated polyimides.

2.4. Synthesis of polymers

A 100 mL, three-necked, round-bottom flask equipped with a mechanical stirrer, a Dean–Stark trap, and a reflux condenser was charged with TFDAS (3.523 g, 10 mmol), HQDPA (4.0231 g, 10 mmol), *m*-cresol (15 mL) containing isoquinoline (2.6 mL), and 35 mL of toluene in nitrogen at room temperature. The mixture was refluxed for 6 h, during which time the water released in the imidization process was removed by distillation as toluene/water azeotrope (Scheme 2). The mixture was then heated to 200 °C and kept there for 12 h. After cooling to room temperature, the solution was diluted with 140 mL of *m*-cresol and then slowly poured into an excess of vigorously stirred ethanol. Solid polymer powder was collected by filtration, washed with ethanol, and then dried at 120 °C for 24 h and 220 °C for 3 h.

IR (KBr): 1780, 1726, 1363, 1320, 1136, 1030 cm^{-1}. ^1H NMR (500 MHz, $CDCl_3$, δ, ppm): 7.95 (d, $J = 8.0$ Hz, 2H), 7.91 (s, 2H), 7.60 (d, $J = 8.5$ Hz, 2H), 7.48 (s, 2H), 7.43 (d, $J = 8.5$ Hz, 2H), 7.41 (d, $J = 8.5$ Hz, 2H), 7.20 (s, 4H).

Polyimide 2 (6FDA/TFDAS), polyimide 3 (ODPA/TFDAS) and polyimide 4 (*s*-BPDA/TFDAS) were synthesized from the polymerization of 1 equiv. of TFDAS and 1 equiv. of 6FDA, ODPA or *s*-BPDA respectively, at 20% solid content in *m*-cresol in the same method as polyimide 1.

Polyimide 2 IR (KBr): 1785, 1731, 1367, 1307, 1141, 1035 cm^{-1}. ^1H NMR (500 MHz, DMSO, δ, ppm): 8.21 (d, $J = 8.0$ Hz, 2H), 8.04 (s, 2H), 7.97 (d, $J = 7.5$ Hz, 2H), 7.78 (d, $J = 8.5$ Hz, 2H), 7.74 (s, 2H), 7.56 (d, $J = 8.5$ Hz, 2H).

Polyimide 3 IR (KBr): 1783, 1728, 1363, 1309, 1133, 1037 cm^{-1}. ^1H NMR (500 MHz, $CDCl_3$, δ, ppm): 8.03 (d, $J = 7.0$ Hz, 2H), 7.91 (s, 2H), 7.60 (d, $J = 8.0$ Hz, 2H), 7.57 (s, 2H), 7.51 (d, $J = 7.0$ Hz, 2H), 7.42 (d, $J = 8.0$ Hz, 2H).

Polyimide 4 IR (KBr): 1782, 1728, 1363, 1305, 1130, 1032 cm^{-1}. ^1H NMR (500 MHz, THF, δ, ppm): 8.62 (s, 2H), 8.51 (d, $J = 6.5$ Hz, 2H), 8.27 (d, $J = 6.5$ Hz, 2H), 8.24 (s, 2H), 7.95 (d, $J = 7.5$ Hz, 2H), 7.69 (d, $J = 8.0$ Hz, 2H).

3. Results and discussion

3.1. Polymer synthesis

The fluorinated polyimides, prepared by a one-step polycondensation procedure, are white to light yellow powders. They were confirmed to be the desired polyimides by FTIR and ^1H NMR spectroscopies. In FTIR spectra, stretching vibrational peaks of C=O, characteristic of polyimides, were found at about 1779–1785 and 1726–1731 cm^{-1}. Peaks corresponding to C–N stretching vibrational were observed at about 1363–1367 cm^{-1} (Fig. 1). The FTIR spectra also reveal the other type of important information: the estimation of the intrinsic optical loss by C–H vibrational absorption. That is the C–H stretching vibration peaks in 3000–3400 cm^{-1} contained information concerning optical loss at visible and near-IR region. If the intensity of the C–H fundamental stretching vibration is strong, the overtone band strength will be increased, and as a result, a large optical loss in the visible and near-IR region would be expected. As shown in Fig. 1, the C–H fundamental stretching vibrations for these polymers were observed to be very low compared to the other peaks, despite the presence of the three C–H bonds on each aromatic ring. This can be attributed to the strong electronic effects of fluorine atoms substituted near the aromatic ring. In ^1H NMR spectra of the resulting polyimides, there were no peaks in the low field below 8.70 ppm, and this indicated complete imidization.

From the GPC data (Table 1), M_w and M_n values were available in the range of 2.15×10^5 to 7.08×10^5 and 1.24×10^5 to 3.21×10^5, respectively. The polydispersity indices M_w/M_n of polyimides were in the range of 1.59–2.20. The results indicate that these polymers have high molecular weights and low polydispersity indices.

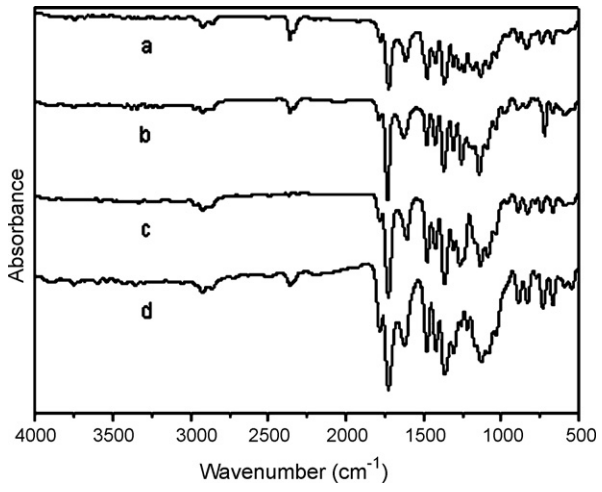

Fig. 1. The IR spectra of the polyimides: (a) polyimide 1, (b) polyimide 2, (c) polyimide 3 and (d) polyimide 4.

Table 1
Properties of the polyimides

Polymer	M_n ($\times 10^5$)	M_w ($\times 10^5$)	M_w/M_n	T_g (°C)	$T_{d,5\%}$ [a] (°C)	$T_{d,10\%}$ [b] (°C)
Polyimide 1	1.43	2.28	1.59	221	561	591
Polyimide 2	3.21	7.08	2.20	269	531	551
Polyimide 3	1.24	2.15	1.73	240	557	590
Polyimide 4	1.35	2.95	2.18	275	556	596

[a] 5% weight loss.
[b] 10% weight loss.

Table 2
Solubilities of polyimides

Polymer	Acetone	Ethanol	Chloroform	*m*-Cresol	THF	DMSO	DMAC
Polyimide 1	−	−	+	+	+	+	+
Polyimide 2	+	−	+	+	+	+	+
Polyimide 3	−	−	+	+	+	+	+
Polyimide 4	+	−	+	+	+	+	+

+: dissolve; −: indissolve.

3.2. Polymer properties

These polymers exhibited very good solubility behavior both in strong aprotic solvents, such as *N*-methyl-2-pyrrolidinone (NMP), DMAc, dimethyl sulfoxide (DMSO), and cyclohexanone, and in common organic solvents, such as THF and *m*-cresol (Table 2). The good solubility is possibly due to the molecular asymmetry structure and the presence of bulk CF_3 groups, which inhibit close packing and reduce the interchain interaction. Another reason is the presence of the flexibilizing ether groups (both –S– group and –O– groups) in the polymer backbone.

The thermal properties of polymers were measured by DSC and TGA, and were listed in Table 1. T_g of the polymers were in the range of 221–275 °C. Due to the effect of a more flexible polymer main-chain structure, the polyimide 1 has the lowest T_g of 221 °C and the polyimide 4 (*s*-BPDA/TFDAS) has the highest T_g of 275 °C because of its rigid polymer main-chain structure. The TGA curves showed 5% and 10% weight loss in the range of 531–561 °C and 551–596 °C, respectively. These imide-containing polymers had higher T_d values due to the incorporation of the thermally stable imide group in the main chain. From both DSC and TGA analyses, it can be confirmed that the polymers have excellent thermal stabilities.

We also study the thermal crosslinking behavior of the polymers. After crosslinking, these polymers show higher thermal stability. Take polyimide 1 as an example, the T_g increases from 221 to 247 °C after cured at 400 °C for 30 min (Fig. 2). TGA analysis was also performed to study the thermal crosslinking behavior of the polymers. As shown in Fig. 3, the 0.5% weight-loss temperature of polyimide 1 increases 52 °C after crosslinking. It is known that high solubility often causes intermixing by solvents between layers by spin-coating. Table 3 shows the solubility of polyimide 1 after crosslinking. This polymer is insoluble when it was crosslinked, so it will not cause intermixing by solvents between layers by spin-coating.

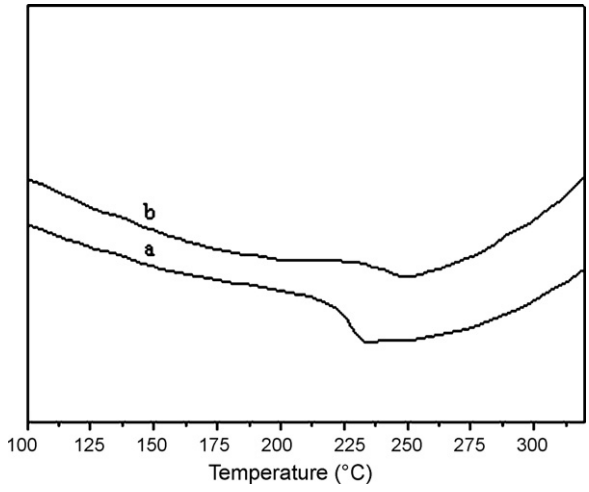

Fig. 2. DSC traces of polyimide 1: (a) before curing and (b) after curing at 400 °C for 30 min.

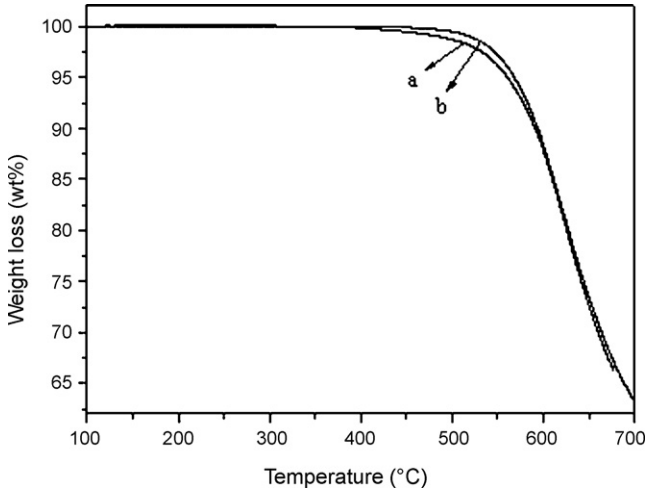

Fig. 3. TGA traces of polyimide 1: (a) before crosslinking and (b) after crosslinking.

Table 3
Solubilities of polyimide 1

Polymer	Acetone	Ethanol	Chloroform	*m*-Cresol	THF	DMSO	DMAC
Polyimide 1 (before curing)	−	−	+	+	+	+	+
Polyimide 1 (after curing)	−	−	−	−	−	−	−

+: dissolve; −: indissolve.

3.3. Optical properties

Fig. 4 shows the UV–vis spectra of polyimides films (45 μm thick). These thick films were prepared by poured polyimides solution onto a glass surface and followed by thermal curing in the following steps: 40 °C/1 h, 80 °C/1 h, 120 °C/1 h, 140 °C/1 h, 160 °C/1 h; after that 150 °C for 30 min in a oven. The UV–vis spectra exhibited the cut-off wavelength at about 370–400 nm. The cut-off wavelength of polyimide 2 (6FDA/TFDAS) is lower than that of the other polyimides. The reason that hexafluoroisopropyl moiety could enhance the transparence of polymer films can be interpreted by the increase in the intermolecular chain distance and the weakness of the intramolecular interaction in the polymer solid state. The cut-off wavelength of polyimide 4 (*s*-BPDA/TFDAS) is the highest because of the tight molecular packing.

Whereas the electronic transition causes the absorption in the UV region, the absorption in the near-infrared region is mainly caused by the harmonics and their coupling of the stretching vibration of chemical bonds. The carbon–hydrogen (C–H) bonds are reported to strongly affect the absorption in the near-infrared region [4,27]. The low absorption in both the 1310 and 1550 nm wavelengths, which are used in optical communications, is an important consideration in using these polymers for optical devices. The absorption in the near-infrared region, therefore, is strongly related to the number of C–H bonds in the polymer. It is also reported that the absorption due to C–H bonds can be reduced by the replacement of hydrogen in the C–H bonds to heavier atoms such as fluorine (F), chlorine (Cl), and deuterium (D). In this issue, considering the price of the material, we partly introduce C–F bonds to replace hydrogen in the C–H bonds. Fig. 5 shows the near-infrared absorption spectra of polyimides films. The first overtone bands (2ν) of the aromatic C–H fundamental vibrations (1ν), the first combination bands ($2\nu + \delta$) of the C–H stretching and bending, and the second overtone bands (3ν) appeared in the region of 2000–1550, 1300–1500 and 1100–1200 nm, respectively. The near-IR spectra would be still difficult to analyze due to a number of overtone and combination bands of various stretching vibrations, for example C–O bonds, C–C bonds, and C=C bonds [4]. The absorption peaks in the region of the first overtones and combination bands were very complicated, but the complexity of the second overtone bands was reduced compared to the lower overtones and combination bands. Based on this point, the effects of fluorination on the C–H vibrational overtones were more clearly observed in the second overtone band region. There is an absorption peak due to the third harmonic of the stretching vibration of the C–H bond (3ν, 1.1 μm), a peak due to the combination of the second harmonic of the stretching vibration and deformation vibration of the C–H bond ($3\nu + \delta$, 1.4 μm), and a peak due to the second harmonic of the stretching vibration of the C–H bond (2ν, 1.65 μm). However, these films have low light absorption at the telecommunication wavelengths of 1.3 and 1.55 μm. Furthermore, the absorption frequency shift also determines the position of the low loss optical windows. Especially for polymer optical fiber (POF) applications, the optical window position should be matched with the optical source for the longer transmission. In the spectra shown in Fig. 5, the wavelengths of the optical telecom source at 1300, 1310, and 1550 nm seem to be quite far from the vibrational frequencies, and absorption at those wavelengths looks negligible, so the polymers are expected to be applicable to optoelectronic materials.

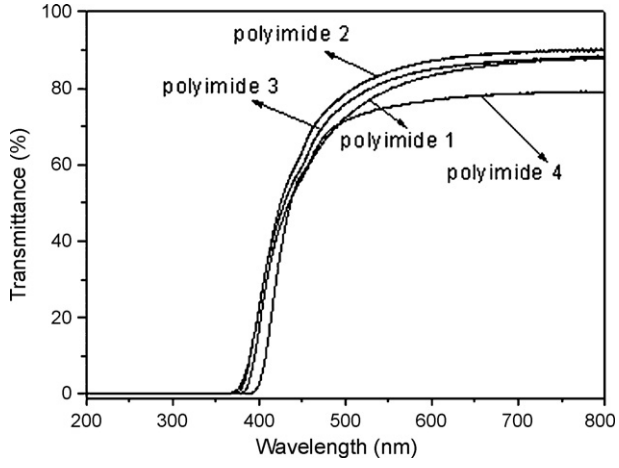

Fig. 4. UV–vis spectrum of polyimides.

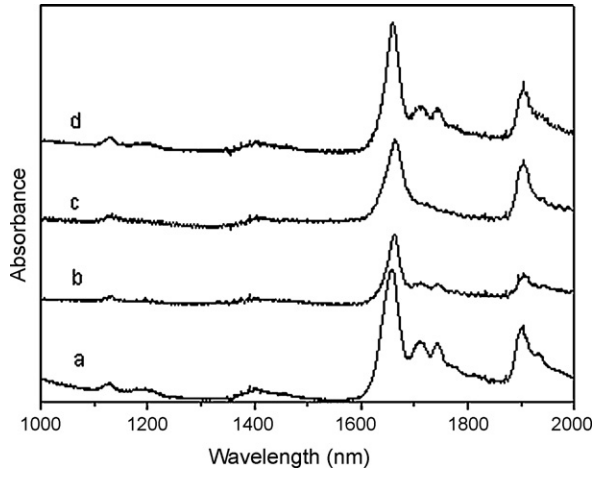

Fig. 5. The optical absorption spectra of polyimides: (a) polyimide 2, (b) polyimide 1, (c) polyimide 4 and (d) polyimide 3.

Table 4
Refractive indices and the moisture absorption of the polyimides films

Polymer	n	n_{TE}	n_{TM}	Δn	Moisture absorption (%)
Polyimide 1	1.619	1.6244	1.6050	0.019	0.7
Polyimide 2	1.5626	1.5722	1.5526	0.019	0.7
Polyimide 3	1.6257	1.6354	1.6034	0.022	0.8
Polyimide 4	1.6380	1.6430	1.5998	0.043	0.8

3.4. Refractive index and birefringence

It is known that the refractive indices, and, therefore, the birefringence in polyimide films are affected by several factors. Main factors include the chain flexibility and linearity, geometry of the repeat units, polarizability and orientation of the bonds in the polymer backbone [28,29]. The in-plane (n_{TE}) and out-of-plane (n_{TM}) refractive indices and the birefringence (the difference between n_{TE} and n_{TM}) of the films are shown in Table 4. The thickness of films was about 1.5 μm. At the room temperature, the refractive indices of the polymers are in the range of 1.5626–1.6380 in 1550 nm. Polyimide 2 had a low refractive index due to the larger aromatic content. As shown in Table 4, the in-plane (n_{TE}) refractive indices are larger than the out-of-plane (n_{TM}). It is due to the rigid aromatic molecules, which tend to align in parallel with the film surface during the film processing. Due to this ordering, light travels slower (higher refractive index) in the in-plane direction compared with the out-of-plane direction. The moisture absorption of the polyimides is lower than 0.8% (Table 4). The polymers exhibited low moisture absorption because of the hydrophobicity of the CF_3 group.

3.5. Fabrication and characterization of rib-type waveguides

The actual waveguide fabrication process is shown schematically in Fig. 6. This optical waveguide was fabricated by spin-coating a core polymer (HQDPA/TFDAS) on an oxidized silicon substrate, and then baked to remove the solvent. Next, the aluminum layer was sputtered onto the core layer and patterned by photolithography. Then a core waveguide was produced using oxygen RIE. Finally, the mask was removed. Fig. 7 shows the top view SEM image of the waveguide. The darker areas represent the ridge of the waveguide. The silica layer of the substrate was identified as the brighter bottom layer. Fig. 8 shows an AFM image of the polymer waveguide. In the 3D micrograph of the pattern, a smooth surface for both the top and sidewall was obtained. From the results of AFM image, it can be observed that the film is about 4 μm thick and the surface roughness of the waveguide beam is less than 5 nm. As shown in Fig. 9, the measurement system of the near-field pattern was based on a tunable semiconductor laser, the tapered fiber and infrared camera. A 1550 nm light from the tunable semiconductor laser was coupled into the waveguides with the tapered fiber. With carefully cleaved samples, the coupling losses between the fiber and the waveguide endface are very repeatable. The output signal was collected and was shown by a monitor. The result is shown in Fig. 10 and it shows the near-field mode pattern of the waveguide (10 μm width), demonstrating a single mode at 1550 nm. This pattern indicates that the optical waveguide operates in a single mode. Details of the waveguide structure and the performance of the optical device will be reported latter.

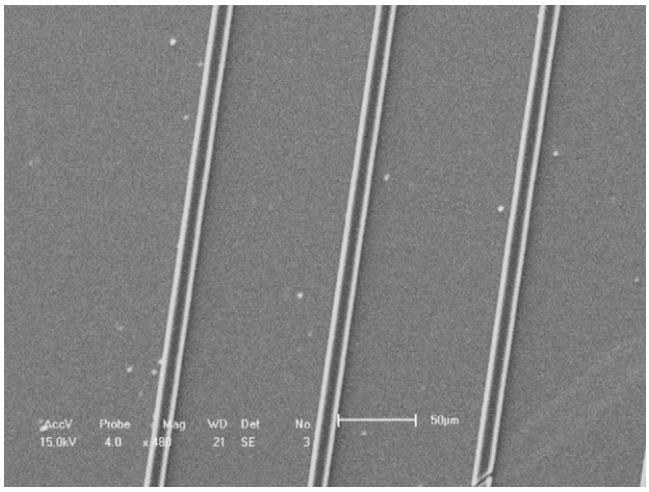

Fig. 7. SEM image of the polyimide 1 (HQDPA/TFDAS).

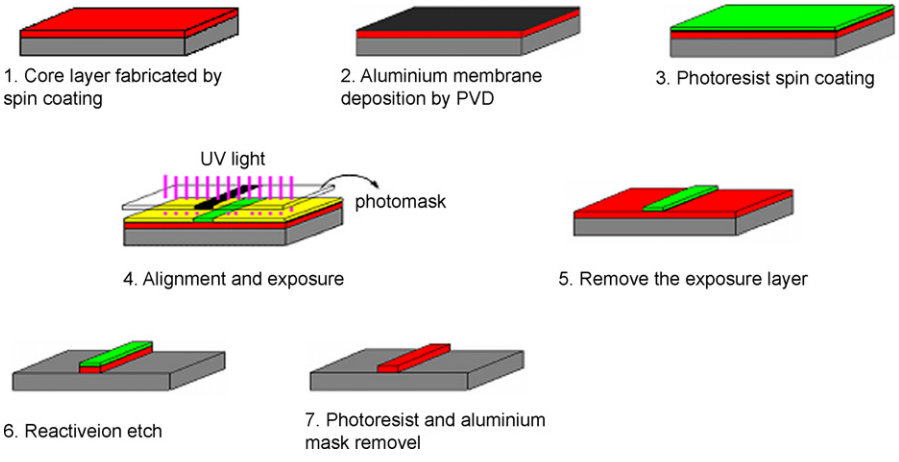

Fig. 6. Schematic diagram of the waveguide fabrication process (, polyimide; , aluminum; , oxidized silicon; and , photoresist).

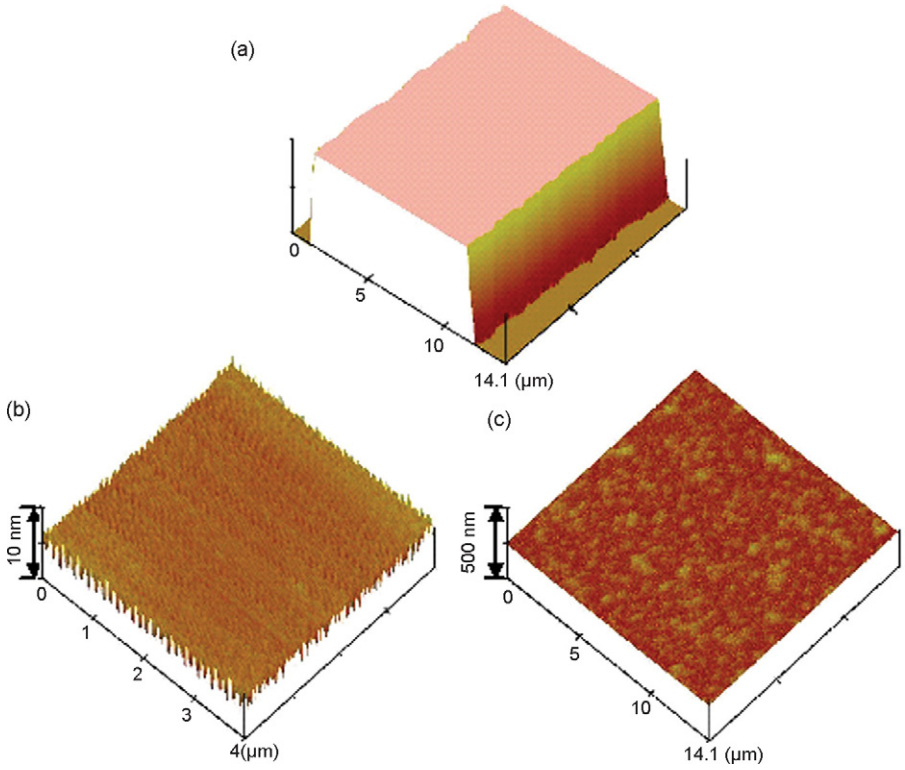

Fig. 8. AFM image of polyimide 1: (a) AFM 3D micrograph of the pattern, (b) surface roughness of the waveguide beam measured by AFM and (c) surface roughness of the silica layer of the substrate measured by AFM.

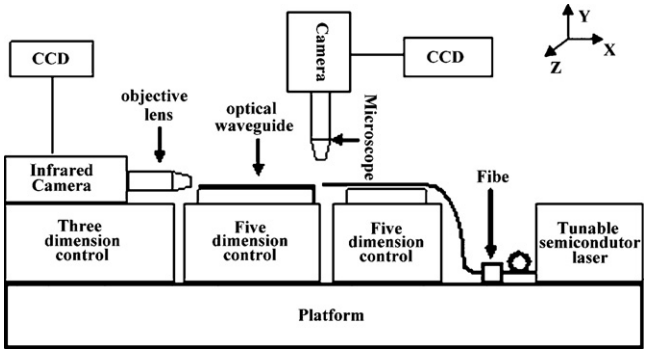

Fig. 9. Measuring system scheme.

Fig. 10. Near-field mode pattern for TE polarized light at 1550 nm.

4. Conclusions

The sul-containing fluorinated polyimides were successfully synthesized by a one-step polycondensation procedure. The chemical structures of polymers were characterized by ^{1}H NMR and FTIR. The polymers exhibit excellent thermal stabilities. T_g of the polymers were between 221 and 275 °C and the 5% weight-loss temperatures were above 531 °C. They have good solubilities in several solvents such as DMAc, THF and *m*-cresol. After crosslinking, these polymers show higher thermal stability and they are insoluble in common solvents. They also have refractive indices of 1.5626–1.638 at 1550 nm and a low water absorption rate about 0.8%. In ultraviolet and visible region, the films of the novel polyimides have a high optical transparency. Rib-type polymeric waveguide device was prepared by using the fluorinated polyimides.

Acknowledgement

The work was supported by the Natural Science Foundation of China (no. 50773025).

References

[1] Y. Zhao, F. Wang, A. Li, B. Liu, Z. Wu, D. Zhang, S. Liu, M. Yi, Mater. Lett. 58 (2004) 2365–2368.
[2] J.W. Kang, J.J. Kim, J. Kim, X. Li, M.-H. Lee, IEEE Photonic Technol. Lett. 14 (2002) 1297–1299.
[3] J. Jiang, L.C. Claire, B. Chantal, S. Jacob, P.N. Julian, J. Ding, Y. Qi, D. Michael, Opt. Mater. 28 (2006) 189–194.

[4] J. Ghim, D.S. Lee, B.G. Shin, D. Vak, D.K. Yi, M.J. Kim, H.S. Shim, J.J. Kim, D.Y. Kim, Macromolecules 37 (2004) 5724–5731.
[5] J.W. Kang, J.P. Kim, W.Y. Lee, J.S. Kim, J.S. Lee, J.J. Kim, J. Lightwave Technol. 19 (2001) 872–875.
[6] M.H. Wei, C.H. Lee, C.C. Chang, W.C. Chena, J. Appl. Polym. Sci. 98 (2005) 1224–1228.
[7] E. Kim, S.Y. Cho, D.M. Yeu, S.Y. Shin, Chem. Mater. 17 (2005) 962–966.
[8] N. Sharma, V.K. Sharma, K.N. Tripathi, Opt. Laser Technol. 39 (2007) 939–945.
[9] V.I. Silin, G.A. Balchytis, J.J. Kulys, J. Biochem. Biophys. Methods 26 (1993) 71–79.
[10] E. Susan, M.L. Steven, B. Peter, S.L. Doris, B.W. Hope, A.E. Joseph, G.G. Dexter, S.D. Larry, E.T. Rebecca, R.B. Richard Jr., E. Wendell, E.V. Timothy, S. Angelina, W.A. William, Adv. Funct. Mater. 12 (2002) 605–610.
[11] D. Kumar, V.K. Sharma, K.N. Tripathi, Opt. Laser Technol. 37 (2005) 397–401.
[12] K. Xie, S.Y. Zhang, J.G. Liu, M.H. He, S.Y. Yang, J. Polym. Sci. Polym. Chem. 39 (2001) 2581–2590.
[13] C.L. Chung, C.P. Yang, S.H. Hslao, J. Polym. Sci. Polym. Chem. 44 (2006) 3092–3102.
[14] S.H. Hslao, Y.M. Chang, H.W. Chen, G.S. Liou, J. Polym. Sci. Polym. Chem. 44 (2006) 4579–4592.
[15] J. Lin, X. Wang, Polymer 48 (2007) 318–329.
[16] O. Nuyken, U. Dahn, W. Ehrfeld, V. Hessel, K. Hesch, J. Landsiedel, J. Diebel, Chem. Mater. 9 (1997) 485–494.
[17] P. Stoll, C. Näther, I. Jeß, W. Bensch, Solid State Sci. 2 (2000) 563–568.
[18] M. Hayashi, A. Ribbe, T. Hashimoto, M. Weber, W. Heckmann, Polymer 39 (1998) 299–308.
[19] T. Matsuura, S. Ando, S. Sasaki, F. Yamamoto, Electron. Lett. 29 (1993) 269–271.
[20] T. Matsuura, S. Ando, S. Matsui, S. Sasaki, F. Yamamoto, Electron. Lett. 29 (1993) 2107–2109.
[21] X. Liu, H. Zhou, Y. Yu, H. Cao, L. Chen, W. Zhang, Polym. Prepr. 44 (2003) 414–415.
[22] Z.H. Gao, T. Ben, X.C. Liu, H. Cao, H. Qiu, C.H. Chen, H.W. Zhou, Z.W. Wu, W.J. Zhang, Polym. Prepr. 41 (2000) 1317–1318.
[23] R.G. Bryant, B.J. Jensen, P.M. Hergenrother, Polym. Prepr. 33 (1992) 910–911.
[24] R.G. Bryant, B.J. Jensen, P.M. Hergenrother, Polym. Prepr. 34 (1993) 513–514.
[25] C. Badarau, Z.Y. Wang, Macromolecules 37 (2004) 147–153.
[26] T.C. WillIiam, A. Nurisayin, J. Am. Chem. Soc. 73 (1951) 5125–5127.
[27] F. Wang, A.Z. Li, W. Sun, Y. Zhao, D.M. Zhang, C.S. Ma, S.Y. Liu, Opt. Mater. 28 (2006) 494–497.
[28] G. Hougham, G. Tesoro, A. Viehbeck, J.D. Chapple-Sokol, Macromolecules 27 (1994) 5964–5971.
[29] G. Hougham, G. Tesoro, A. Viehbeck, Macromolecules 29 (1996) 3453–3456.